aspects are clear. As the concentration of nickel is increased, the material crystallizes in lattices with progressively greater fractions of face-shared octahedral structures. One would expect that ultimately a 2H lattice would be adopted since pure RbNiCl$_3$ has the 2H structure. At this time we have no estimate of the minimum concentration of nickel necessary to produce a 2H phase. It is possible, however, that magnesium ion has only a limited solubility in a 2H lattice. Other divalent ions such as V(II) and Co(II) which have 2H-RbMCl$_3$ structures might be expected to produce structural modifications in RbMgCl$_3$ similar to those caused by Ni(II). The fact that Mn(II) does not cause lattice modifications seems reasonable since pure RbMnCl$_3$ adopts a 6H structure.

The EPR spectra clearly show that Mn(II) impurities readily enter both magnesium sites in 4H- and 9R-RbMgCl$_3$. The relative intensities, however, indicate that the distribution of Mn(II) ions between the two sites is not precisely statistical. In 6H-RbMgCl$_3$ there are two type 2 sites for each type 1 site, but the Mn(II) concentration in types 1 and 2 appear to be nearly equal. In 9R-RbMgCl$_3$ there are two type 2 sites for each type 3 site, but the Mn(II) concentration in type 2 is approximately 3 times that in type 3. Although the Mn(II) ions discriminate between sites, the level of selectivity is relatively small. This observation is consistent with earlier studies on doped CsCdCl$_3$ crystals where Mn(II) was found to be less selective with respect to different lattice sites than either V(II) or Ni(II).[14]

Finally, it should be noted that the 2H phase of RbMgCl$_3$ reported by Tishura and co-workers[7] was never encountered in our investigations. There is some indication that the material which they characterized actually had a 4H or 6H structure. The lattice constant reported for the *c* axis is 5.936 Å which is smaller than the *c* axis of CsMgCl$_3$, 6.187 Å,[18] by more than 0.2 Å. If the lattice constants of a number of known 2H lattices (CsVCl$_3$, RbVCl$_3$, CsCoCl$_3$, RbCoCl$_3$, CsNiCl$_3$, RbNiCl$_3$)[19–22] are considered, it appears that the *c* dimensions of the rubidium salts are only about 0.03 Å smaller than those of the corresponding cesium salts. The value of 5.936 Å is almost exactly one-half of the *c* dimension of 4H-RbMgCl$_3$ and one-third of the *c* dimension of 6H-RbMgCl$_3$. It is possible that Tishura and co-workers did not properly index the X-ray powder pattern from the RbMgCl$_3$ which they prepared.

(19) R. W. Asmussen, T. K. Larsen, and H. Soling, *Acta Chem. Scand.*, **23**, 2055 (1969).
(20) H. J. Seifert and P. Ehrlich, *Z. Anorg. Allg. Chem.*, **302**, 284 (1959).
(21) H. Soling, *Acta Chem. Scand.*, **22**, 2793 (1968).
(22) A. Engberg and H. Soling, *Acta Chem. Scand.*, **21**, 168 (1967).
(23) G. N. Tischenko, *Tr. Inst. Kristallogr., Akad. Nauk SSSR*, **11**, 93 (1955).

Contribution from Ames Laboratory—DOE and Department of Chemistry, Iowa State University, Ames, Iowa 50011

Synthesis by Hydrogen-Driven Disproportionation Reactions. Synthesis and Structure of the Hexazirconium Dodecahalide Clusters Zr$_6$Cl$_{12}$ and Zr$_6$Br$_{12}$ and the Double Salt Zr$_6$Cl$_{12}$·M$_2$ZrCl$_6$ (M = Na, K, Cs)

HIDEO IMOTO, JOHN D. CORBETT,* and ALAN CISAR

The ZrXH phases, X = Cl, Br, formed by reaction of H$_2$ with double-metal-layered ZrX at 150–450 °C are metastable and decompose at 630–780 °C to ZrH$_2$ plus the cluster compound Zr$_6$X$_{12}$, the latter being isostructural with Zr$_6$I$_{12}$. Transport of Zr$_6$Cl$_{12}$ occurs in the sealed Ta container at about 800 °C. The two cluster phases are also formed as powders from incomplete reactions of ZrX and ZrX$_4$ at 650–700 °C, while the layered 3R-ZrCl$_2$ is more stable at lower temperatures. Decomposition of ZrClH in the presence of NaCl, KCl, or CsCl at 750 °C yields the isostructural M$_2$Zr$_7$Cl$_{18}$ (M = Na, K, Cs) while ZrCl does not react with NaCl or KCl alone under the same conditions. The crystal structure of the double salt K$_2$Zr$_7$Cl$_{18}$ was solved by single-crystal diffractometer methods ($R\bar{3}$, a = 9.499 (2) Å, c = 25.880 (6) Å, R = 0.037, R_w = 0.049, 736 Mo Kα diffractions corrected for absorption). The structure contains the octahedral metal cluster Zr$_6$Cl$_{12}$ slightly compressed along the $\bar{3}$ axis [d(Zr–Zr) = 3.224 (1), 3.178 (1) Å] and edge bridged by chlorine. Halides in octahedral ZrCl$_6^{2-}$ groups occupy all exo positions of the clusters. The structure can also be described in terms of nine chlorine layers per cell containing regular potassium and vacancy substitutions together with zirconium(II) and zirconium(IV) in octahedral interstices. The Zr$_6$Cl$_{12}$ and Na$_2$Zr$_7$Cl$_{18}$ phases quenched in the presence of hydrogen at ~1 atm do not contain hydrogen in the clusters.

Introduction

Zirconium monochloride and monobromide provided the first two examples of a new and novel structure type, namely, infinite sheets of strongly bonded double-metal layers sandwiched between double-halogen layers,[1–3] the structures of ZrCl and ZrBr differing only in packing details of the four-layer slabs. The zirconium monohalides were subsequently both found to react with hydrogen quite readily to form distinct hemihydride and monohydride phases,[4] and the magnitudes of the enthalpy changes for these reactions together with

chemical reasoning suggested that the strongly bound hydrogen is located in the electron-rich region between the double-metal layers. Subsequent NMR studies[5,6] have indicated that the hydrogen is probably distributed principally among the tetrahedral interstices between the metal layers.

The initial motivation for the present research came from a desire to grow single crystals of ZrXH$_{0.5}$ (X = Cl, Br). Although the heavy-atom positions in ZrXH$_{1.0}$ have recently been deduced from X-ray powder data,[7] it has not been possible to solve the lower symmetry structure of the hemihydride

(1) Troyanov, S. I. *Vestn. Mosk. Univ., Ser. 2: Khim.* **1973**, *28*, 369.
(2) Adolphson, D. G.; Corbett, J. D. *Inorg. Chem.* **1976**, *15*, 1820.
(3) Daake, R. L.; Corbett, J. D. *Inorg. Chem.* **1977**, *16*, 2029.
(4) Struss, A. W.; Corbett, J. D. *Inorg. Chem.* **1977**, *16*, 360.

(5) Hwang, T. Y.; Torgeson, D. R.; Barnes, R. G. *Phys. Lett. A* **1978**, *66A*, 137.
(6) Murphy, P. D.; Gerstein, B. C. *J. Chem. Phys.* **1979**, *70*, 4552.
(7) Daake, R. L.; Corbett, J. D., unpublished research.

in this way. Better crystals of the parent monohalides have been made by synthesis at higher temperatures than originally reported,[2,8] and so the same approach was tried with the hemihydride by utilizing values of the hydrogen-dissociation pressures extrapolated to higher temperatures. In fact the halohydrides were found to be unstable under these conditions with respect to ZrH_2 and Zr_6X_{12}, thereby providing a much better synthetic route to single crystals of these two cluster halides than previously known. The cluster Zr_6I_{12} has been previously identified as one of three phases near ZrI_2 in composition in a system where the monohalide evidently does not exist.[9,10] The cluster chloride was first obtained in powdered form in studies of the $ZrCl_2$ system (3R-type layered structure)[11] and was identified as being isostructural with Zr_6I_{12}.

Another aspect of the present study derived from recent discoveries in this laboratory that new cluster halides may also be stable as anions, for example, in phases for which simple representations are $Sc^{3+}Sc_6Cl_{12}^{3-}$,[9] $(ScCl_2^+)_\infty(Sc_4Cl_6^-)_\infty$,[12] and $Cs^+(Nb_6I_{11}^-)$.[13] The decomposition of ZrClH was therefore carried out in the presence of CsCl, KCl, and NaCl, reactions which afforded not a new cluster but a novel phase $M_2Zr_7Cl_{18}$ with M = Cs, K, Na.

Experimental Section

Synthesis. As in other recent studies,[3,9,11-13] all reactions were carried out in tantalum tubes which had been sealed by arc welding under ≤ 0.5 atm of He. These were in turn jacketed in evacuated and sealed fused silica tubes to protect them from oxidation. Starting materials were synthesized as before,[3] and standard high-vacuum and drybox techniques were employed in their handling. Hydrogen used for the syntheses was 99.999% H_2 (Matheson). CsCl, KCl, and NaCl were dried under dynamic vacuum at 350 °C.

Hydrogenation Apparatus. The apparatus for hydrogen reactions previously described[4] had the sample contained in a Mo boat in a long fused silica tube closed at the end which projected into a cylindrical furnace. The other end was connected through a Hoke metal valve to the vacuum line and measuring apparatus. A temperature limit of ~400 °C for the published equilibrium studies of H_2 reactions with ZrCl and ZrBr was dictated principally by the irreversible disproportionation caused when the autogenous equilibrium pressure of $ZrX_4(g)$ above the solid phases diffused from the heated zone and condensed, leaving small amounts of ZrH_2 admixed with the sample. This problem was completely avoided in the present study through use of a sealed Ta container for the sample as this conveniently functions as a semipermeable membrane for H_2.[14] The container remains in the α or interstitial-phase region at all the temperatures and pressures involved, and above about 650 °C the rate of hydrogen transfer well exceeds the usual rate with which hydrogen reacts with a number of inorganic solids of interest.[15]

The conditions for typical H_2 reactions studied and the products formed are listed in Table I. As described before[11] phases were identified by Guinier powder techniques (Model XDC-700 camera, IRDAB, Stockholm) utilizing NBS Si as an internal standard. For precise lattice constant determinations the positions of the zero and Si reference lines were related to their θ values by a quadratic in distance utilizing standard least-squares methods. Powder patterns for δ- and ε-ZrH_2 were taken from the literature.[16]

$K_2Zr_7Cl_{18}$: Crystal Selection and Data Collection. The crystal used for data collection had an approximate shape of a parallelepiped with ill-formed faces; the overall size was 0.24 × 0.15 × 0.12 mm. The crystal was sealed in a 0.2 mm i.d., thin-walled capillary in a nitrogen atmosphere within the drybox and mounted on a four-circle dif-

(8) Struss, A. W.; Corbett, J. D. *Inorg. Chem.* **1970**, *9*, 1373.
(9) Corbett, J. D.; Daake, R. L.; Poeppelmeier, K. R.; Guthrie, D. H. *J. Am. Chem. Soc.* **1978**, *100*, 652.
(10) Guthrie, D. H.; Corbett, J. D., unpublished research.
(11) Cisar, A.; Corbett, J. D.; Daake, R. L. *Inorg. Chem.* **1979**, *18*, 836.
(12) Poeppelmeier, K. R.; Corbett, J. D. *J. Am. Chem. Soc.* **1978**, *100*, 5039.
(13) Imoto, H.; Corbett, J. D. *Inorg. Chem.* **1980**, *19*, 1241.
(14) Franzen, H. F.; Khan, A. S.; Peterson, D. T. *J. Less-Common Met.* **1977**, *55*, 143.
(15) Imoto, H.; Corbett, J. D. *Inorg. Chem.*, in press.
(16) Mueller, W. M.; Blackledge, J. P.; Libowitz, G. G., Eds. "Metal Hydrides"; Academic Press: New York, 1968; pp 268-9.

Table I. Some Reactions of the Zirconium Monohalides with Hydrogen and Alkali Metal Chlorides

solid reactants (amt, g)	H_2 pressure, atm	$T, °C^a$	t, days	products
Zr (strips, excess), $ZrCl_4$ (0.050)	2	$610/700^b$	30	Zr_6Cl_{12}, Zr_6Cl_{15} powders covering hydrided metal, considerable $ZrCl_4$
ZrCl (0.36)	2	690	25	Zr_6Cl_{12}, $ZrClH_x$, ZrH_2, trace of $ZrCl_4$
ZrCl (0.54) (cool end)	1	780/810	22	Zr_6Cl_{12} crystals (wall); ZrH_2, Zr_6Cl_{12}, $ZrClH_x$ (residue)
ZrCl(1) (cool end)	1	630/710	10	Zr_6Cl_{12}, ε-ZrH_2, $ZrClH_x$ (substantially no transport)
ZrBr (0.5)	0.53	750	32	Zr_6Br_{12}, δ- and ε-ZrH_2, trace of $ZrBrH_x$
ZrCl (0.58), KCl (0.14)	0.53	750	20	$K_2Zr_7Cl_{18}$, K_2ZrCl_6, ε-ZrH_2
ZrCl (0.91), NaCl (0.081)	1	750/740	12	$Na_2Zr_7Cl_{18}$, ZrH_2 (Na_2ZrCl_6)
ZrCl (0.70), KCl (0.080)	0	702	4	ZrCl, KCl
ZrCl (0.68), NaCl (0.138)	0	850	16	ZrCl, NaCl

^{a} Quenched with water unless otherwise noted; under H_2 when present with reaction tube disconnected from apparatus. ^{b} Cooled slowly, keeping $P(H_2)$ just above that calculated for $ZrClH_{0.5}$.[3]

fractometer designed and built in the Ames Laboratory. The procedures used for indexing and orientation of the crystal have been described previously.[17] The cell parameters and reflection data showed that the crystal belongs to the rhombohedral space group. X-ray data were collected at ambient temperature with the use of Mo Kα radiation monochromatized with a graphite single crystal (λ = 0.71002 Å). All reflections within a sphere defined by $2\theta \leq 50°$ in octants HKL and $H\bar{K}L$ (hexagonal axes) were examined with use of an ω-scan mode. Peak heights of three standard reflections which were remeasured every 75 reflections to check the instrument and crystal stability did not show any change over the data collection period. Final cell parameters and their estimated standard deviations were obtained from least-squares refinement of 16 reflections tuned on the diffractometer with the same crystal giving a = 9.499 (2) Å and c = 25.880 (6) Å.

Structure Determination and Refinement. Programs for data reduction, structure solution and refinement, and illustration have been referenced before.[18] Data reduction yielded 1272 reflections ($I \geq 3\sigma(I)$) from 1372 possible reflections. Averaging of duplicate reflections yielded 737 independent data. The lack of any systematic absence other than that for R centering was consistent only with space groups $R\bar{3}$ and $R3$, and the former was assumed for further work. The positions of Zr1 and all chlorine atoms were determined from a Patterson map. Other atoms were located from a Fourier map. The full-matrix least-squares refinement with anisotropic thermal parameters proceeded uneventfully to convergence at R = 0.039 and R_w = 0.054, where $R = \sum(|F_o| - |F_c|)/\sum|F_o|$, $R_w = [\sum w(|F_o| - |F_c|)^2/\sum w|F_o|^2]^{1/2}$, and $w = \sigma_F^{-2}$. The reflection data were then corrected for absorption, the shape of crystal being approximated with six faces. The volume absorption coefficient was 46.2 cm^{-1}, and the transmission factors ranged from 0.529 to 0.597. Data reduction and averaging now yielded 736 independent reflections. Full-matrix least-squares refinement on the corrected data set converged at R = 0.038 and R_w = 0.061. Because weaker reflections were observed to have larger values of $w\Delta^2$ ($\Delta = |F_o| - |F_c|$), the data set was

(17) Jacobson, R. A. *J. Appl. Crystallogr.* **1976**, *9*, 115.
(18) Adolphson, D. G.; Corbett, J. D.; Merryman, D. J. *J. Am. Chem. Soc.* **1976**, *98*, 7234.

reweighted in ten groups sorted according to F_o so that $w\Delta^2$ values for all the groups were the same. The final residuals were $R = 0.035$ and $R_w = 0.047$. Scattering factors for Zr^{2+} (an average of Zr and Zr^{4+}), Zr^{4+}, Cl^-, and K^+ were used for Zr1, Zr2, Cl, and K atoms, respectively, and corrections for the real and imaginary parts of anomalous dispersion were included.[19] The final difference Fourier synthesis map was flat to ± 1.0 e/$Å^3$, and, in particular, no peak was found in the center of the cluster.

Results

Zr_6X_{12} Clusters. The red-brown chloride Zr_6Cl_{12} is formed directly in $ZrCl-ZrCl_4$ reactions but not very efficiently under the conditions sampled. The usual products in this composition range are its polymorph, the 3R form of the layered $ZrCl_2$, and, on slight reduction, an evidently large number of ordered, substoichiometric compositions of related structure.[11] The cluster chloride was first found as a powder from isothermal equilibrations of $ZrCl-ZrCl_4$ samples with overall compositions Cl/Zr between 1.95 and 2.00 at and above 650 °C, with better yields above 700 °C. The X-ray pattern was successfully indexed as a Zr_6I_{12} type[9] ($R\bar{3}$, $a = 12.973$ (1) Å, $c = 8.782$ (1) Å) as shown in Table II. Positional parameters for the intensity calculations were estimated by modifying those for the cluster in $Sc^{3+}Sc_6Cl_{12}^{3-}$ (which has the same structure save for the isolated cation[20]) to produce the same bond distances found in Zr_6Cl_{15}.[9] The existence of a reciprocity failure with the strongest reflections observed was established by multiple exposures, so the pattern was scaled such that $\sum I_o = \sum I_c$. The observed pattern also contained four weak ($I \leq 3/100$) lines and one strong (29/100, 1.3767 Å) line, which could only be assigned to unknown impurities; these were not observed in the sample obtained by the following method.

Decomposition of ZrX with H_2 at 700–800 °C (Table I) is a better route to Zr_6X_{12}, X = Cl, Br, according to the reaction

$$12ZrX(s) + 6H_2(g) \rightarrow Zr_6X_{12}(s) + 6ZrH_2(s)$$
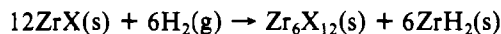
Volatile halides, especially an equilibrium pressure of ZrX_4 above ZrX of 5–50 torr[21] which would ordinarily be lost with an open sample, are retained by the sealed tantalum reaction vessel which still readily passes hydrogen. Synthesis of the cluster in situ from $ZrCl_4$ and Zr in the presence of H_2 is slow and incomplete, as is customary for reactions with metal,[3] and synthesis starting with the more reactive ZrCl near 700 °C gives the product admixed with ZrH_2 and sometimes ZrClH. However near 800 °C black gemlike crystals of Zr_6Cl_{12} ca. 0.3 mm in diameter are obtained on the wall, presumably through a slow transport in a small temperature gradient. Better results were obtained when the reaction container was quenched.

A similar reaction of ZrBr with H_2 gives Zr_6Br_{12}. The indexing of its powder pattern on the Zr_6I_{12} structure is shown in Table III. The remaining lines from this preparation are only three from ZrBrH and seven from δ- (upper limit) and ε-ZrH_2 (lower limit). On the basis of this identification, the cluster Zr_6Br_{12} can also be established as a hitherto unidentified intermediate in $ZrBr_4-ZrBr$ reactions. The usual final product in this composition range (750 °C, 10 days) is apparently the layered 2H-$ZrBr_2$,[11] but intermediate term reactions (e.g., 650 °C, 7 days) generate Zr_6Br_{12} mixed with $ZrBr_3$ and unreacted ZrBr. A very good pattern which is in

excellent agreement with calculated intensities (Table III) was obtained after removing the $ZrBr_3$ and unreacted $ZrBr_4$ from this product through rapid washing with acetone or 10% methanol in trichloroethylene followed by vacuum drying.[21]

The lattice constants for Zr_6Cl_{12} and Zr_6Br_{12} prepared under different conditions and by different routes are listed in Table IV. The first three examples illustrate the reproducibility of the hydride route for Zr_6Cl_{12} and the powder data analysis. In addition, the data are of interest regarding the possible insertion of hydrogen into the clusters since increases in lattice dimensions during such hydrogen incorporation into the Nb_6I_8 clusters in Nb_6I_{11}[22,23] and $CsNb_6I_{11}$[13] can be readily discerned by Guinier techniques. Although no change in lattice constants

Table II. Observed and Calculated Powder Patterns for Zr_6Cl_{12}

d(obsd), Å	d(calcd), Å[a]	hkl	I(obsd)[b]	I(calcd)[c]
6.95	6.92	101	34[d]	68
6.51	6.49	110	23	31
4.10	4.09	012	9	13
3.826	3.823	211	10	12
3.751	3.745	300	11	14
3.486	3.460	202	2	0.2
3.254	3.243	220	11	13
3.055	3.052	122	11	14
2.939	2.937	131	5	7
2.669	2.668	11$\bar{3}$	7	12
2.543	2.541	13$\bar{2}$	46[d]	100
2.473	2.473	321	10	9
2.452	2.452	140	8	10
2.367	2.366	042	9	9
2.307	2.306	303	3	4
2.224	2.223	232	12	14
2.176 {	2.177	05$\bar{1}$	16	12
	2.173	22$\bar{3}$		
2.156	2.155	104	14	11
2.064	2.064	241	13	9
2.000	2.000	502	4	4
1.966	1.967	511	4	2
1.950	1.950	214	2	1
1.912	1.912	24$\bar{2}$	5	6
1.880	1.880	143	7	6
1.835	1.834	152	5	3
1.799	1.799	520	30	33
1.794	1.795	134	29	32
1.680	1.682	161	3	2
1.622	1.623	125	6	3
1.598	1.596	612	2	2
1.578	1.579	351	3	2
1.571	1.570	054	2	1
1.533	1.533	523	7	2
1.526	1.526	244	4	4
1.506	1.507	35$\bar{2}$	10	2
1.4889	1.4881	710	9	4
1.4683	1.4683	262	15	16
1.4638	1.4637	006	4	5
1.4510	1.4514	23$\bar{5}$	4	5
1.4184	1.4185	44$\bar{3}$	5	2
1.4151	1.4155	630	5	5
1.3262	1.3265	173	6	5
1.3104	1.3101	27$\bar{2}$	3	3
1.3004	1.3005	81$\bar{1}$	2	2
1.2961	1.2957	53$\bar{4}$	3	4
1.2738	1.2743	633	11	8
1.2705	1.2706	62$\bar{4}$	13	14
1.2514	1.2511	37$\bar{1}$	5	4
1.2155	1.2147	372	4	3
1.1374	1.1375	912	12	16
1.1352	1.1354	526	10	17

[a] $R\bar{3}$, $a = 12.973$ (1) A, $b = 8.782$ (1) A. [b] Scaled such that $\sum I_o = \sum I_c$. [c] Estimated crystal parameters: Zr, 0.159, 0.043, 0.149 (0.8 A^2); Cl1, 0.127, 0.174, 0.332 (1.5 A^2); Cl2, 0.310, 0.228, 0.000 (1.5 A^2). [d] Overexposed; reciprocity failure.

(19) "International Tables for X-ray Crystallography"; Kynoch Press: Birmingham, England, 1968, 1974; Vols. III, IV.

(20) The Zr_6I_{12} structure and the isostructural Zr_6Cl_{12} and Zr_6Br_{12} are most conveniently compared with $K_2Zr_7Cl_{18}$ and other structures when the clusters are centered at the origin. The published parameters for Zr_6I_{12}[9] are transformed to this basis as follows: Zr, $y - x - 1/3$, $y - 2/3$, $z - 1/6$; I_1 and I_2, same as Zr plus inversion or ($2/3$, $1/3$, $1/3$), respectively. The data for Sc(Sc$_6$Cl$_{12}$)[9] require Sc1 and Cl1, $1/3 - x$, $2/3 - y$, $1/6 - z$ and Sc2 and Cl2, $x - y$, x, $1/2 - z$ to place the cluster at the origin.

(21) Daake, R. L. Ph.D. Thesis, Iowa State University, 1976.

(22) Simon, A. *Z. Anorg. Allg. Chem.* **1967**, *355*, 311.

(23) Simon, A., private communication, 1979.

Table III. Observed and Calculated Powder Patterns for Zr_6Br_{12}[a]

d(obsd), Å	d(calcd), Å[b]	hkl	I(obsd)[c]	I(calcd)[d]
7.24	7.29	101	15	37
6.75	6.79	110	10	13
4.95	4.97	021	2	2
4.310	4.319	012	10	11
4.001	4.009	211	10	6
3.912	3.919	300	10	10
3.395	3.394	220	15	9
3.212	3.211	122	10	8
3.094	3.096	003	2	9
3.076	3.077	131	30	30
2.816	2.817	113	10	12
2.669	2.669	13$\bar{2}$	100[e]	150
2.590	2.590	321	10	7
2.565	2.566	410	10	12
2.484	2.484	402	10	9
2.428	2.429	303	2	3
2.331	2.332	232	15	10
2.285	2.287	223	5	5
2.278 {	2.280	051	20	15
	2.278	104		
2.161	2.161	241, 024	20	10
2.100	2.100	502	2	2
2.060 {	2.060	511	2	2
	2.058	214		
2.005	2.004	422	5	4
1.976	1.976	143	5	6
1.892	1.892	134	45	52
1.883	1.883	520	50	55
1.770	1.771	205	2	1
1.615	1.614	315	2	7
1.607 {	1.609	523	30	24
	1.606	621		
	1.605	244		
1.580	1.580	532	2	3
1.557	1.557	710	5	3
1.547	1.548	006	5	9
1.539	1.538	262	30	30
1.531	1.530	235	2	5
1.487 {	1.488	443	2	4
	1.486	541		
	1.486	434		
1.482	1.482	630	5	4
1.4198 {	1.4196	271	2	2
	1.4192	164		
1.3725	1.3724	722	2	4
1.3612 {	1.3614	811	2	6
	1.3610	354		
1.3348 {	1.3363	633	30	32
	1.3348	461		
	1.3344	624		
1.3100	1.3097	731	2	4
1.2227 {	1.2219	651, 91$\bar{1}$	10	15
	1.2216	274		
1.1961	1.1957	526	30	30
1.1916 {	1.1914	912	30	35
	1.1905	327		

[a] Sixteen lines with I(obsd) ≤ 1/100 omitted; all but one assignable to Zr_6Br_{12}. [b] $R\bar{3}$, a = 13.577 (1) Å, c = 9.287 (1) Å. [c] Scaled to medium lines. [d] Estimated positional parameters: Zr, 0.153, 0.043, 0.140; Br1, 0.312, 0.231, 0.001; Br2, 0.126, 0.178, 0.325. B = 0.3 Å² for all. [e] Reciprocity failure.

occurred when Zr_6Cl_{12} prepared from ZrClH was heated to 600 °C in high vacuum, the significantly smaller dimensions and molar volumes found for both clusters when prepared without hydrogen (6–11 Å³ (12–22σ) or 0.4–0.9% in volume) suggest tightly bound hydrogen may be present which could not be so removed, as with that in $Nb_6I_{11}H$.[22] The absence of hydrogen in the clusters was however established by pulsed NMR techniques as recently employed in the study of ZrXH.[6] In particular 5000 scans on ca. 50 mg of Zr_6Cl_{12} crystals revealed only a broad Lorenzian-shaped line (fwhm = 36 kHz). The breadth of the resonance contrasts with that expected for weak dipolar coupling of well-separated and im-

Table IV. Comparison of Lattice Constants for Zr_6Cl_{12} and Zr_6Br_{12} Prepared by Different Methods

reactants (conditions[a])	no. of reflctns fitted	lattice constants		molar vol, Å³
		a, Å	c, Å	
ZrCl + H_2 (700 °C, 1 atm, 4 d)	29	13.009 (1)	8.813 (2)	1291.6 (4)
ZrCl + H_2 (630 °C, 1 atm, 10 d; 600 °C, hvac, 2 h)	28	13.003 (2)	8.814 (4)	1290.6 (7)
ZrCl + H_2 (745 °C, 1 atm, 9 d)	27	13.005 (1)	8.808 (1)	1290.2 (3)
ZrCl + $ZrCl_3$ (700 °C, 26 d)	50	12.973 (1)	8.782 (1)	1280.0 (3)
Δ(av)		0.033 (2)	0.030 (3)	10.8 (5)
ZrBr + H_2[b]	41	13.577 (1)	9.287 (1)	1482.7 (4)
ZrBr + $ZrBr_3$ (650 °C, 7 d)	29	13.563 (1)	9.269 (1)	1476.7 (3)
Δ		0.014 (2)	0.018 (2)	6.0 (5)

[a] d = days and hvac = high vacuum. [b] See Table I.

mobile protons such as the 0.6 kHz wide signal found with $CsNb_6I_{11}H$.[24] The observation with Zr_6Cl_{12} corresponds to approximately 4 wt % ZrH_2 contamination and has a line width comparable to that obtained with a larger sample of $Na_2Zr_7Cl_{18}$ known to contain ZrH_2 (41 kHz) and a hydrogen-richer sample of $ZrH_{1.9}$ (55 kHz).

A very small amount of nonstoichiometry is a plausible, alternate explanation for the observed shift in lattice dimensions, the larger constants belonging to a more reduced $Zr_{6+x}Cl_{12}$, which is in equilibrium with ZrH_2. The $ZrCl–ZrCl_4$ reactions are characteristically incomplete and probably in more facile equilibrium with $ZrCl_4$. Introduction of a small amount of Zr^{n+} in the Zr_6X_{12} structure at $(0, 0, ^1/_2)$ together with the addition of its n electrons to neighboring clusters would be an attractive but unproven possibility, analogous to the way in which the structure of $Sc(Sc_6Cl_{12})$ differs from that of Zr_6Cl_{12} (vide infra). Though these end members can readily be distinguished by Guinier intensity measurements, the very small amount of nonstoichiometry necessary to accomplish the observed lattice contraction cannot. The crystal of Zr_6I_{12} studied[9] was probably near the oxidized limit and showed no evidence of extra or displaced atoms in any interstice.

Consistent with the foregoing tentative conclusions regarding both hydrogen content and nonstoichiometry are the facts that neither Zr_6Cl_{12} from a $ZrCl–ZrCl_4$ reaction nor $Na_2Zr_7Cl_{18}$ prepared by the $ZrCl–H_2$ route (below) gives a significant ESR signal at room temperature or 77 K. On the other hand, Zr_6Cl_{12} from the $ZrCl–H_2$ reaction does show a very broad signal of reasonable strength at both temperatures that is not easily interpreted. Quantitative susceptibility measurements with the present samples do not seem feasible.

The Double Salt $Zr_6Cl_{12}·K_2ZrCl_6$. If KCl is present during the $ZrCl–H_2$ reaction, a new black product is formed, $K_2Zr_7Cl_{18}$ according to crystallographic analysis, by the reaction

$$16ZrCl(s) + 2KCl(s) + 9H_2 \rightarrow K_2Zr_7Cl_{18}(s) + 9ZrH_2(s)$$
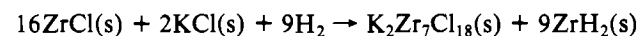
With excess KCl and hydrogen there is further disproportionation, viz.

$$K_2Zr_7Cl_{18}(s) + 6 KCl(s) + 3H_2 \rightarrow$$
$$4K_2ZrCl_6(s) + 3ZrH_2(s)$$
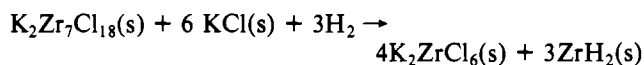
The isostructural $Na_2Zr_7Cl_{18}$ may be obtained by an analogous reaction as judged by both Guinier and zero-level Weissenberg photographs of the product. The isostructural relationship between $Cs_2Zr_7Cl_{18}$ and the potassium salt was established by comparison of several dozen intensities measured from a single

(24) Barnes, R. G., private communication, 1980.

Table V. Positional and Thermal Parameters for $Zr_6Cl_{12} \cdot K_2ZrCl_6{}^a$

	x	y	z	$B_{11}{}^b$	B_{22}	B_{33}	B_{12}	B_{13}	B_{23}
Zr1	0.050 86 (6)	0.216 37 (6)	0.049 78 (2)	1.16 (3)	1.18 (3)	0.97 (3)	0.59 (2)	−0.02 (1)	−0.05 (1)
Zr2	0.0	0.0	0.5	1.14 (4)	B_{11}	0.95 (5)	$B_{11}/2$	0.0	0.0
K	0.0	0.0	0.224 05 (15)	5.31 (11)	B_{11}	3.86 (16)	$B_{11}/2$	0.0	0.0
Cl1	0.240 09 (18)	0.184 33 (17)	0.113 45 (5)	2.10 (6)	1.82 (6)	1.34 (6)	1.16 (5)	−0.64 (4)	−0.48 (4)
Cl2	0.428 39 (17)	0.137 71 (17)	0.002 41 (5)	1.22 (6)	1.70 (6)	1.64 (6)	0.69 (5)	0.06 (4)	0.35 (4)
Cl3	0.103 25 (17)	0.476 07 (17)	0.111 68 (5)	1.71 (6)	1.60 (6)	1.54 (5)	0.78 (5)	−0.45 (4)	−0.50 (4)

^{a} Additional data: $K_2Zr_7Cl_{18}$; $Z = 3$; rhombohedral; $R\bar{3}$ (No. 148); $a = 9.499$ (2) Å; $c = 25.880$ (6) Å; $R = 0.037$ and $R_w = 0.049$ (736 reflections). ^{b} $T = \exp[-0.25(B_{11}h^2a^{*2} + B_{22}k^2b^{*2} + B_{33}l^2c^{*2} + 2B_{12}hka^*b^* + 2B_{13}hla^*c^* + 2B_{23}klb^*c^*)]$.

Table VI. Important Distances (Å) and Angles (Deg) in $Zr_6Cl_{12} \cdot K_2ZrCl_6{}^a$

Distances^b

Zr1–Zr1^i	3.224 (1)	Cl1–Cl1^{ii}	3.581 (3)
Zr1–Zr1^{ii}	3.178 (1)	Cl1–Cl1^{iv}	3.381 (2)
Zr1–Cl1	2.566 (2)	Cl1–Cl2	3.528 (2)
Zr1^i–Cl1	2.574 (2)	Cl1–Cl3	3.602 (2)
Zr1^i–Cl2	2.544 (2)	Cl1^{ii}–Cl3	3.535 (2)
Zr1^i–Cl2^{ii}	2.546 (2)	Cl1–Cl3^v	3.553 (2)
Zr1–Cl3	2.770 (2)	Cl2–Cl2^{vi}	3.503 (2)
Zr2^{iii}–Cl3	2.474 (2)	Cl2–Cl2^{vii}	3.600 (2)
K–Cl1	3.530 (3)	Cl2^{viii}–Cl3	3.508 (2)
K–Cl1^{iv}	3.564 (2)	Cl2^{vii}–Cl3	3.592 (2)
K–Cl2^{iv}	3.468 (3)	Cl3–Cl3^v	3.493 (2)
K–Cl3^v	3.663 (2)	Cl3–Cl3^i	3.506 (2)

Angles

Zr1–Zr1^{ii}–Zr1^i	60.95 (2)	Cl3–Zr2^{iii}–Cl3^v	89.78 (5)
Zr1–Cl2^{viii}–Zr1^{vii}	77.28 (4)	Zr1–Cl3–Zr2^{iii}	133.15 (6)
Zr1–Cl1–Zr1^i	77.69 (5)	Zr1^{vi}–Zr1–Cl3	178.2 (1)

^{a} Symmetry operations coded as: (i) $y - x$, $\bar{x}$, z; (ii) y, $y - x$, $\bar{z}$; (iii) $^1/_3 + x$, $^2/_3 + y$, $-^1/_3 + z$; (iv) $^2/_3 - x$, $^1/_3 - y$, $^1/_3 - z$; (v) $^2/_3 + x - y$, $^1/_3 + x$, $^1/_3 - z$; (vi) $\bar{x}$, $\bar{y}$, $\bar{z}$; (vii) $x - y$, x, $\bar{z}$; (viii) $\bar{y}$, $x - y$, z. ^{b} Only Cl–Cl distances below 3.61 Å are listed; the cut-off on all others is 4.0 Å.

crystal on the diffractometer with those calculated with the positional parameters of $K_2Zr_7Cl_{18}$ (below); the lattice constants for $Cs_2Zr_7Cl_{18}$ are $a = 9.595$ (1) and $c = 26.186$ (8) Å.

The driving force for all of these disproportionation reactions must be the formation of ZrH_2, since ZrCl shows no reaction when heated alone with either KCl (4 days, 702 °C) or NaCl (16 days, 850 °C) (Table I).

Structure Description. Final positional and thermal parameters for $K_2Zr_7Cl_{18}$ are listed in Table V while the more important distances and angles are given in Table VI. Observed and calculated structure factors are available as supplementary material.

The ternary compound is constituted as $Zr_6Cl_{12} \cdot K_2ZrCl_6$, the chlorine in $ZrCl_6{}^{2-}$ anions occupying all the exo or outward-directed positions from Zr1 atoms in the cluster. The cluster has $\bar{3}$ crystallographic symmetry and contains an approximate metal octahedron in which all edges are bridged by "inner" chlorine atoms (Figure 1). The unit is distorted from rigorous O_h symmetry by a trigonal compression which makes Zr–Zr distances around the waist 0.046 Å less than those between atoms related by the threefold axis. The bridging chlorine atoms are disposed nearly symmetrically but with metal–chlorine distances involving the six Cl1 atoms at the top and bottom slightly longer (by 0.015 Å, 5σ) than the six Cl2 atoms around the waist (Figure 1); thus the former do not completely "follow" the trigonal compression.

Longer Zr1–Cl3 bonds link each cluster to six separate $ZrCl_6{}^{2-}$ ions. The environment around a single $ZrCl_6{}^{2-}$ anion is shown in Figure 2. Though the anion has only $\bar{3}$ crystallographic symmetry, it is very close to the ideal octahedral; moreover the chlorine atoms therein are displaced by only 1.8° from the ideal exo position of the cluster. Potassium occurs in somewhat large cavities with 12 nearest chlorine neighbors
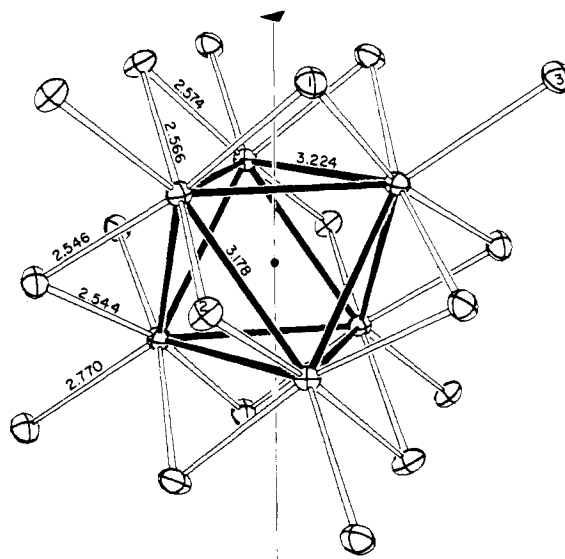
Figure 1. The Zr_6Cl_{12} cluster in $Zr_6Cl_{12} \cdot K_2ZrCl_6$ together with the six outer Cl3 atoms from neighboring $ZrCl_6$ groups ($\bar{3}$ symmetry, 50% probability thermal ellipsoids).
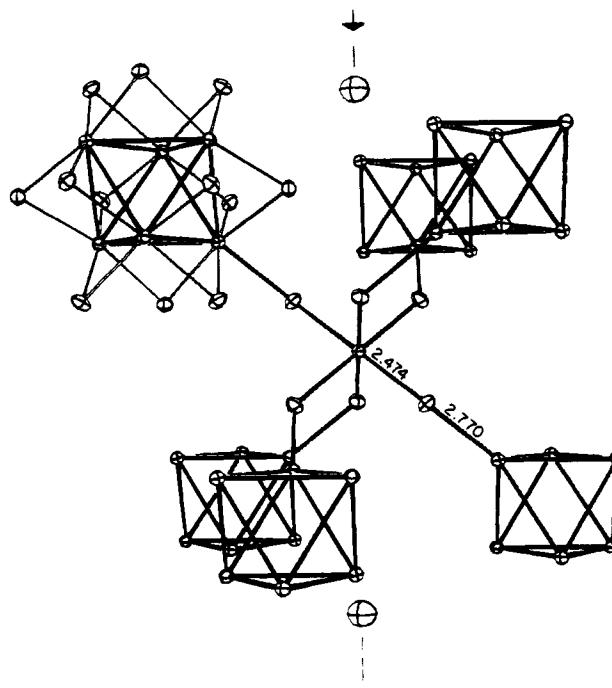
Figure 2. The bonding of the $ZrCl_6{}^{2-}$ ions to six Zr_6Cl_{12} clusters in $K_2Zr_7Cl_{18}$. The isolated atoms are potassium (50% probability thermal ellipsoids, c axis vertical).

at 3.47–3.66 Å compared with the van der Waals sum of 3.14 Å. Only one slightly short chlorine–chlorine distance occurs, 3.38 Å between Cl1 atoms in separate clusters which are linked by $ZrCl_6{}^{2-}$ anions.
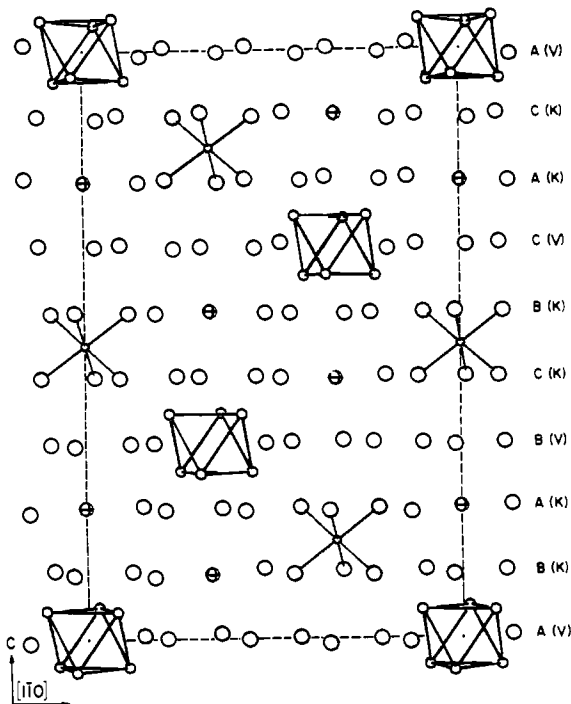
Figure 3. The [110] projection of the structure of $Zr_6Cl_{12}\cdot K_2ZrCl_6$. The Zr_6 clusters and the $ZrCl_6^{2-}$ ions are outlined. Open circles are chlorine; crossed circles are potassium; both are of arbitrary size. See text for an explanation of the layer notation on the right-hand side.

The overall structure of $Zr_6Cl_{12}\cdot K_2ZrCl_6$ can be described in two useful ways. The first is in terms of cubic-close-packed Zr_6Cl_{12} clusters with their threefold axes normal to the layers. In this arrangement K^+ occupies all the tetrahedral holes and $ZrCl_6^{2-}$ all of the octahedral holes, the chlorine atoms in the latter being bonded to the six clusters which define each interstice.

A more novel and striking description comes from the viewpoint of the chlorine array, as illustrated in Figure 3 in a (110) section of the structure. The chlorine atoms occur in close-packed layers sequenced ...ABABCBCAC... or as $(chh)_3$ in terms of neighboring layers.[25] As shown in Figure 4 there are seven chlorine atoms in each layer in the unit cell so that substitutions are based on sevenths. Pairs of chlorine layers hh each have one-seventh of the chlorine atoms replaced by potassium (K), and the third layer has one of seven chlorine positions vacant (V). In terms of the substituents K and V, the layers are now sequenced $A(V)$ $B(K)$ $A(K)$ $B(V)$ $C(K)$ $B(K)$ etc. or $c(V)h(K)h(K)$.... Finally one-seventh of the octahedral holes between potassium-substituted (h) layers, those which are defined only by chlorine, are occupied by zirconium(IV) while three-sevenths of the octahedral holes between layers ch, namely, those which surround a chlorine vacancy, are occupied by zirconium(II) atoms to produce the clusters. The R-centering operation applied sequentially to the layers ABA (chh) will be seen to generate the same results (Figure 3). The relationship of the unit cells in $K_2Zr_7Cl_{18}$ and Zr_6X_{12} is shown in Figure 4 in terms of the ideal close-packed layers.

The foregoing type of description in terms of close-packed layers and regular vacancies with metal atoms in octahedra is not unique to just the cluster compound $Zr_6Cl_{12}\cdot M_2ZrCl_6$. Considerable similarities among other cluster halides are found when these are considered from this viewpoint, for example in Zr_6X_{12} (X = Cl, Br, I[9]), M_7X_{12} (Sc_7Cl_{12},[9] La_7I_{12},[26] etc.) and M_6X_{14} (Nb_6Cl_{14},[27] Ta_6I_{14}[28]). In the first two the ccp
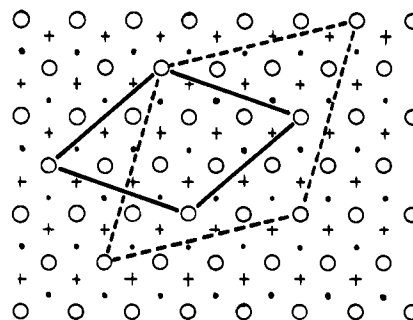
Figure 4. Projection of close-packed chlorine layers along z axis, with unit cells of $K_2Zr_7Cl_{18}$ (solid line) and Zr_6X_{12} (dashed line) indicated. Symbols O, •, and + refer to A, B, and C layers, respectively, in Figure 3 without substitutions or introduction of vacancies.

halide layers have one in 13 chlorine atoms missing, namely, those in the center of the M_6 cluster. In the second type, M_7X_{12}, one additional metal atom per cluster occupies an octahedral hole, similar to Zr2 in $K_2Zr_7Cl_{18}$, but along the $\bar{3}$ axis of the cluster. And in the M_6X_{14} examples where the halide layers are ordered ABAC $[(ch)_2]$, the C layers only have 25% vacancies. Half of these occur in the center of the metal clusters; the remainder appear to be generated by requirements of the bridging chlorine atoms.

Discussion

The metal–metal distances found for Zr_6Cl_{12} in $K_2Zr_7Cl_{18}$, 3.224 (1) and 3.178 (1) Å, compare favorably with those in Zr_6I_{12}, 3.204 (2) and 3.195 (1) Å, respectively,[9] in spite of the difference in connectivity between the clusters. A substantial matrix effect from the larger iodide does not seem evident. The foregoing metal–metal distances are also close to the average in the hcp metal, 3.205 Å. The cluster in $K_2Zr_7Cl_{18}$ achieves greater symmetry since all 12 chlorine atoms only bridge edges, the exo positions being occupied by chlorine from the $ZrCl_6^{2-}$ anion, while in the binary halide the cluster also has $\bar{3}$ local symmetry, but the six bridging halogens about the waist also occupy exo positions in neighboring clusters.

Though magnetic studies have not yet clarified ground-state configurations of these clusters, the observed distortions and bridging modes suggest that they will be diamagnetic, at least at low temperatures. Evidently the best measure of the ordering of the bonding molecular orbitals in M_6X_{12} clusters comes from calculations and optical measurements on $Nb_6X_{12}^{n+}$ and $Ta_6X_{12}^{n+}$ by Robbins and Thomson.[29] They concluded that the metal–metal bonding levels were, in order of decreasing energy, a_{1g} (z^2), t_{1u} $(z^2) \simeq t_{1u}$ (xz, yz), and a_{2u} (xy), the same order that is obtained with a one-electron extended Hückel calculation on the Zr_6X_{12} clusters.[30] This ordering would produce a paramagnetic result for an octahedral cluster such as Zr_6Cl_{12} since there would be only four electrons in the second t_{1u} level. However, the degeneracy of this is suitably altered to e_u (more bonding) and a_{2u} by either of the observed effects, that is, a trigonal compression as in $Zr_6Cl_{12}\cdot K_2ZrCl_6$ or a smaller compression together with use of the waist halide to bridge to other clusters as occurs in Zr_6X_{12}.

The present findings demonstrate that the ZrXH phases, X = Cl, Br, are only metastable with respect to ZrH_2 and ZrX_2, specifically the cluster form of the dichloride Zr_6X_{12}, by the reaction

(25) Wells, A. F. "Structural Inorganic Chemistry", 4th ed.; Oxford University Press: Oxford, England, 1975; p 131.
(26) Warkentin, E.; Berroth, K.; Simon, A., unpublished research.

(27) Simon, A.; von Schnering, H.-G.; Wöhrle, H.; Schäfer, H. *Z. Anorg. Allg. Chem.* **1965**, *339*, 155.
(28) Bauer, D.; von Schnering, H.-G.; Schäfer, H. *J. Less-Common Met.* **1965**, *8*, 388.
(29) Robbins, D. J.; Thomson, A. J. *J. Chem. Soc., Dalton Trans.* **1972**, 2350.
(30) Corbett, J. D., unpublished research, 1979.

$$12ZrXH(s) \rightarrow 6ZrH_2(s) + Zr_6X_{12}(s)$$

Incorporation of hydrogen into the strongly bound double-metal layers in the monohalide can be accomplished at low enough temperatures (150–450 °C) that more stable alternatives are not accessible. The fact that the hydrogen dissociation pressure over the two ZrXH phases is about 700 times that above ZrH_2 (at 400 °C[4]) would suggest that decomposition would ensue if bonding of the halide and the remaining zirconium in the halide product were anything like that in the reactant. Evidently Zr_6X_{12} clusters fulfill this role better than the alternate, layered ZrX_2 structure at temperatures necessary for decomposition. The layered $ZrCl_2$ is known to be a filled-band semiconductor, each metal having six neighbors at 3.39 Å compared with four at about 3.20 Å in the cluster. The total Zr–Zr bond order per metal is then greater in the cluster, but the number of Zr–Cl interactions is less, and the layered $ZrCl_2$ appears to be the more stable form below about 650 °C. (Actually most of the earlier synthetic experiments with layered dihalides which were pertinent to this transformation involved the more common, substoichiometric $Zr_{1+x}X_2$ phase[11] for which disproportionation is also involved in the (unfavorable) conversion to Zr_6X_{12}.) The cluster becomes more stable at higher temperatures, consistent with an X-ray density which is 11% lower (for the chloride) principally because of the vacancy in the middle of the cluster.

The evident simplicity of the cluster syntheses via ZrXH appears to depend at least in part on the predetermined stoichiometry therein. Another advantage is that the equilibrium is reached through states with lower partial pressures of ZrX_4, which makes it possible to heat the system at higher temperature from the beginning and avoid the formation of other phases stable only at lower temperatures. In contradistinction, ZrX–ZrX_4 reactions, which must be heated slowly to avoid excessive ZrX_4 pressures, tend to produce mixtures of phases which are not at equlibirium, particularly in the region ZrX–$Zr_{1+x}X_2$,[3,11] while the more oxidized systems ZrX_2–ZrX_3 generate unusual pressures at the necessary temperatures, e.g., about 27 atm at 600 °C for X = Cl.[31] Ordinarily the zirconium monohalides are stable to disproportionation to temperatures[3] well in excess of the stability region for the cluster compounds. However, the introduction of hydrogen into the system drastically alters the free energy balance by stabilizing the metal through the formation of zirconium hydrides. At 1 atm of H_2 the free energy of formation of ZrH_{2-x} is estimated to be –46, –33, and –22 kJ/mol at 600, 700, and 800 °C, respectively, from integration of the area between the isotherm and $P = 1$ atm in the published dissociation pressure data.[32]

(31) Daake, R. L.; Corbett, J. D. *Inorg. Chem.* **1978**, *17*, 1192.
(32) Reference 16, p 247.

Contribution from the Department of Chemistry,
University of California, Davis, California 95616

Crystal Structures and Properties of Bis(2,5-dithiahexane)copper(I) and -copper(II) and Mixed-Valence Complexes. Comparison of Tetrahedral and Distorted Octahedral Geometries of Thioether-Coordinated Copper(II)

MARILYN M. OLMSTEAD, W. KENNETH MUSKER,* and RICHARD M. KESSLER

X-ray diffraction results are reported for the series of complexes $Cu^I(2,5\text{-}DTH)_2ClO_4$, $Cu^I_2Cu^{II}(2,5\text{-}DTH)_6(ClO_4)_4$, and $Cu^{II}(2,5\text{-}DTH)_2(ClO_4)_2$ (2,5-DTH = 2,5-dithiahexane). The copper(I) and mixed-valence salts are isomorphous and crystallize in the cubic space group $I\overline{4}3d$ with $a = 17.214$ (1) and 17.273 (2) Å, respectively. The mixed-valence salt contains crystallographically equivalent copper(I) and copper(II) and is more correctly formulated as $Cu(2,5\text{-}DTH)_2(ClO_4)_{4/3}$. Both the copper(I) and mixed-valence salts have 12 copper atoms per unit cell but differ in the number of perchlorates: 12 for the copper(I) salt and 16 for the mixed-valence salt. The copper atom is tetrahedrally surrounded by a thioether S_4 donor set. The copper(II) salt crystallizes in the space group $P2_1/n$, with $a = 8.249$ (3) Å, $b = 10.185$ (4) Å, $c = 11.169$ (3) Å, $\beta = 108.26$ (2)°, and $Z = 2$. The geometry of the copper(II) complex is distorted octahedral, involving a square-planar S_4 donor set and semicoordination to axial perchlorate groups. This series of complexes allows comparisons to be made between the two common geometries of copper without adjusting for a change in ligands. Interestingly, the Cu–S distance is observed to lengthen as copper(I) oxidizes: $Cu(2,5\text{-}DTH)_2ClO_4$, 2.263 (6); $Cu(2,5\text{-}DTH)_2(ClO_4)_{4/3}$, 2.27 (2); $Cu(2,5\text{-}DTH)_2(ClO_4)_2$, 2.320 (1), 2.354 (1) Å. As the geometry changes from distorted octahedral to tetrahedral, the position of the $S(\sigma) \rightarrow Cu^{II}$ charge transfer is red shifted only ca. 400 cm^{-1}.

Introduction

Crystal structures of copper(I) and copper(II) complexes with the metal coordinated to the same ligands or groups of ligands have received considerable attention for what they may reveal about structural changes accompanying oxidation and reduction of copper in metalloenzymes.[1–3] In none of the structures reported to date is the environment around copper kept as fixed upon loss or gain of an electron as it is likely to

(1) (a) Dockal, E. R.; Diaddario, L. L.; Glick, M. D.; Rorabacher, D. B. *J. Am. Chem. Soc.* **1977**, *99*, 4530. (b) Glick, M. D.; Gavel, D. P.; Diaddario, L. L.; Rorabacher, D. B. *Inorg. Chem.* **1976**, *15*, 1190. 14-ane-S_4 = 1,4,8,11-tetrathiacyclotetradecane.